A METHOD FOR CRYSTALLOGRAPHIC TEXTURE INVESTIGATIONS USING STANDARD X-RAY EQUIPMENT

Mark D. Vaudin[1], Martin W. Rupich[2], Martha Jowett[2], G.N. Riley, Jr.,[2] and John F. Bingert[3]

[1]NIST, Ceramics Division, Gaithersburg, MD 20899.

[2]American Superconductor Corp., Two Technology Drive, Westborough, MA 01581.

[3]Los Alamos National Lab, Materials Technology, Los Alamos, NM 87545.

ABSTRACT

A fast and accurate method has been developed for measuring crystalline texture in homogeneous materials. The method uses a conventional powder x-ray diffractometer capable of θ scans. Two scans are recorded from the sample: first, a high resolution θ-2θ scan is obtained of a Bragg peak whose diffracting planes are normal to the preferred orientation direction; second, a θ scan is obtained using this peak. The θ scan contains the required texture information but the intensities must be corrected for defocussing and absorption to obtain the texture profile. The θ-2θ scan of the Bragg peak is used to make the defocussing correction, and first principles calculations are used to correct for absorption. The theory behind these corrections is presented here. The validity of the technique has been verified by making measurements on untextured alumina. Data obtained from $Bi_2Sr_2Ca_2Cu_3O_{10}$ superconducting tape specimens with this technique are compared with texture data obtained with a four-circle diffractometer.

I. INTRODUCTION

It is frequently desirable, in both applied and basic research, to be able to perform rapid, accurate texture measurements. For example, during the development of a product where

crystallographic texture plays an important role in the performance of the product, it is necessary to assess the effects of different manufacturing processes on texture and to correlate the observed texture with measured properties. To date, accurate texture measurements have required specialized equipment not available in most laboratories. However, many laboratories have access to conventional powder x-ray diffractometers, and this paper describes a technique that uses such a diffractometer and is both fast and accurate.

The work reported in this paper is concerned with texture that is axisymmetric about a single sample axis, also known as fiber texture. The texture axis (fiber axis) is a specimen direction, such as the normal to a flat specimen or the axis of a rod-shaped specimen. Extensions to this work will consider more complex textures. To describe the axisymmetric texture of a crystalline phase in a specimen, we specify the preferred crystallographic direction, i.e. the crystal direction preferentially aligned with the texture axis. In order to quantify a fiber texture, diffraction techniques are typically used to measure the volume fraction of the specimen whose preferred crystallographic direction is at a certain angle to the fiber axis. This angle corresponds to the angle of specimen tilt, α, used below. If the texture of a specimen is measured over all of orientation space, the texture can be expressed as multiples of a random distribution (MRD) by dividing the specimen volume fraction at a particular orientation by the volume fraction of a random specimen that is at that same orientation. If the range of orientation space that can be measured is experimentally limited, as in the rocking curve technique presented here, the texture cannot be expressed in MRDs, but the shape of the texture distribution over the range measured can be determined.

As an example of an application where texture is an important material property, we will consider silver-clad superconducting $Bi_2Sr_2Ca_2Cu_3O_{10}$ (BSCCO 2223) tapes. The electrical and mechanical properties of these tapes are strongly affected by the crystallographic texture developed during the manufacturing process. BSCCO 2223 has an orthorhombic crystal structure with $a \approx b \approx 0.54$ nm, $c \approx 3.72$ nm $\approx 7a$ (JCPDS card 46-0780 [1]), and the equilibrium grain shape is typically platelike and lamellar, with [001] normal to the plates. During the thermomechanical processing of the tape (which involves drawing, rolling and swaging) the (001) planes in the grains become preferentially aligned parallel to the plane of the tape. The texture of the BSCCO 2223 tapes has the following characteristics: it is primarily axisymmetric (fiber texture), the normal to the plane of the tape is the fiber axis and the (001) pole is the preferred crystallographic direction. The critical current density (J_c)

in the whole family of BSCCO superconductors is typically highly anisotropic. In BSCCO 2212, single crystal work has determined that the a and b directions have J_c values 2 to 3 orders of magnitude greater than the c direction [2]. Work on superconducting 2223 tapes has shown that the (001) texture described above aligns the grains in the best orientation for carrying current and is required in applications where current-carrying capacity is the main concern [3].

As discussed above, in addition to accuracy and speed, the texture measurement technique requires a conventional x-ray powder diffractometer with only two specimen rotation axes, as opposed to the more sophisticated equipment required to do complete texture determinations, where the specimen can be rotated about three independent axes. Methods that use peak intensities from conventional θ-2θ spectra have been commonly used to measure texture in materials. In one of these methods the intensities of Bragg peaks from the planes normal to the texture axis are compared with peaks from planes at different angles to the texture axis [4]; this method yields semi-quantitative data at best. A second, more quantitative, method is Rietveld analysis of powder diffraction patterns in which a diffraction pattern calculated from various model functions is fitted to an experimentally obtained pattern. The method can be used to measure texture by incorporating into the refinement a model function that contains one or more refinable parameters describing sample texture [5]. For 2223 tapes, even moderate (001) texture in the plane of the tape results in a conventional θ-2θ scan that only contains peaks of the form 002n (where n is a positive integer), because all the significant diffracting planes other than (001) are tilted more than 40° from (001), and this severely limits the applicability of these two techniques. In addition, in the Rietveld technique the texture is only measured at α values (angles from the texture axis) equal to the angles between the preferred crystallographic direction and normals to diffracting crystal planes, which means that for high symmetry crystal structures there are only limited data.

In light of the above considerations, a rocking curve technique has been developed that involves measuring the intensity of a Bragg peak whose diffracting planes are normal to the preferred crystallographic direction, while tilting (rocking) the specimen. However, when the specimen is tilted out of the symmetric diffraction orientation, only the rotation axis of the specimen remains in focus, i.e. with the scattering angle equal to the Bragg angle. The scattering angle at all other positions on the specimen varies, affecting the measured intensities; this phenomenon is known as defocus. Various defocus correction methods have been devised for use with texture goniometer experiments. One

approach uses intensities measured from randomized specimens, but such specimens are difficult to make, especially for platelike materials such as BSCCO. Other correction methods assume that the Bragg peak used for the texture measurement has a Gaussian intensity distribution [6, 7]. The new method for measuring texture described in this paper explicitly determines the intensity distribution of the texture measurement Bragg peak with a high resolution θ-2θ scan, and uses this profile to correct the intensities of the Bragg peak measured during a θ scan. Two scans are recorded from the sample: a θ scan using the texture Bragg peak, and a high resolution θ-2θ scan of the intensity profile of this peak. The validity of the technique has been assessed by measuring the texture of a randomly oriented alumina powder prepared by spray drying. In addition, selected BSCCO 2223 tape specimens have been characterized using this technique and compared with texture measured using pole figure data collected with a four-circle diffractometer.

II. EXPERIMENTAL PROCEDURE

The technique presented in this paper requires the collection of two x-ray intensity scans using a conventional powder x-ray diffractometer, capable of both symmetric θ-2θ scans (Bragg-Brantano), and θ scans. Several diffractometers were used during this work so that results from different machines could be compared. The results presented in this paper were obtained using a Siemens D500 diffractometer equipped with a focusing Ge incident beam monochromator tuned to Cu $K\alpha_1$ radiation. However, monochromatic radiation is not a requirement for this technique. (Commercial equipment is identified in order to adequately describe the experimental procedure; this does not imply a recommendation or endorsement by NIST, nor does it imply that the equipment is necessarily the best available for the purpose.) Typically, fixed incident slit geometry was used in the experiments, as opposed to fixed irradiated area geometry (theta-compensating slits). The technique requires that the divergence of the incident beam (or the spot size) be the same for both scans, and that the beam divergence (or spot size) be accurately known. Also, the final slit size must be the same for both scans. No anti-scatter slits are placed on the detector side of the diffractometer as they intercept x-rays diffracted from a specimen tilted out of the symmetric position (i.e. during a θ scan) and affect the recorded intensities. The presence in the beam path of Soller slits parallel to the diffraction plane does not affect the measurements beyond reducing the intensity.

The BSCCO 2223 superconducting tape specimens were 12 mm sections of BSCCO

monofilaments encased in silver. The tapes were about 0.25 mm thick and 3 mm wide, and the width of the superconducting monofilament was about 1.5 mm. The tapes were prepared for x-ray analysis by etching the silver from one side of the tape in a mixture of ammonium hydroxide and hydrogen peroxide. After etching, the tape was mounted on a small glass slide using double-stick tape.

The first scan is a relatively high resolution θ-2θ scan over a preferred orientation peak; in the case of BSCCO, the peak used was 0024. The scan should extend far enough that both ends of the scan have a flat background; typically, a scan of 4° in 2θ was all that was required. It was important that the recorded intensity profile be smooth, and the 2θ step size and recording time were set accordingly, with more intense peaks requiring shorter recording times. In the BSCCO experiments 0.01° steps and 10 s times were used; subsequent experiments with 0.02° steps and shorter times (~4 s) showed little if any reduction in data quality. The center of the peak, $2\theta_o$, was measured (this could be determined by eye to the nearest 0.01°) and the second scan was performed, a θ scan with the scattering angle set to $2\theta_o$ and θ scanned from $-\theta_o + 5°$ to $\theta_o - 5°$. For this scan, called herein the rocking curve, the step size was determined by the texture of the specimen; for example, a highly textured specimen required a smaller step size because the rocking curve intensity varies more rapidly with θ. In these experiments the θ step size was 0.25° and the recording time was 10 seconds. To reduce the length of the irradiated area in the diffraction plane, and thereby reduce the corrections that were applied to the rocking curve intensities, the incident beam divergence for both scans was set to the smallest size that produced, in a reasonable period of time, intensity data with sufficiently high signal to noise for the analysis. The final slit divergence for both scans was relatively large to encompass as much of the diffracted beam as possible, thus increasing the recorded intensity. Typically, in the BSCCO experiments the incident slit divergence was 0.68° and the final slit divergence was 0.15°, although other slit sizes were successfully used.

The peak profile and rocking curve data were analyzed using software based on theory developed in the next section. In order to determine how accurately this analysis described the defocusing that occurs during collection of the rocking curve data, various θ-2θscans were collected from untextured alumina with the specimen offset from the symmetric position by a fixed angle. These θ-offset scans were obtained using a strong Bragg peak, 03$\underline{3}$0 (50% of maximum in JCPDS card 10-173 [1]), that had a relatively high Bragg angle (68.2°). Theta offsets of -15° and 15° were used with a variety of incident and final slit sizes. In addition, corrected rocking curves were obtained from the

untextured alumina, to investigate whether they displayed the expected constant level of intensity.

For comparison with the rocking curve data from the BSCCO specimens, pole figure data were collected from the BSCCO specimens using the Schulz reflection technique on a Huber four-circle goniometer with Fe-Kα radiation. In addition, chi scans were performed on the same equipment.

III. THEORY OF DATA ANALYSIS TECHNIQUE

The intensity data, I_m, measured during the two scans described above are functions of scattering angle (2θ) and specimen tilt (α) away from the symmetric condition, and are split into signal, I, and background components as follows:

general case: $I_m = I(2\theta, \alpha) + I_b(2\theta, \alpha)$

(1) for the θ-2θ scan (peak profile) $I_m = I(2\theta, 0) + I_{pb}(2\theta, 0)$ (1)

(2) for the θ scan (rocking curve) $I_m = I(2\theta, 0) + I_{pb}(2\theta, 0)$

where θ_o is the Bragg angle of the peak used in the rocking curve scan. The first step in data analysis is the subtraction of background intensity from the peak profile and rocking curve, leaving the signal intensities, which will be called reduced intensities. The peak profile is collected over a small 2θ range; the background, $I_{pb}(2\theta, 0)$, is assumed to be linear over this range, and is obtained by averaging the background intensities over two 2θ ranges well to each side of the peak and fitting a straight line through the two average intensities. The background contribution to the rocking curve, $I_{rb}(2\theta_o, \alpha)$, is assumed to be equal to $I_{pb}(2\theta_o, 0)$ corrected for changes in the volume of specimen with which the x-rays interact as α varies. This change in interaction volume is described by a factor, $V(2\theta_o, \alpha)$, such that:

$$I_{rb}(2\theta_o, \alpha) = \frac{I_{pb}(2\theta_o, 0)}{V(2\theta_o, \alpha)}. \quad (2)$$

The theory in this section will be developed for the more usual case where a constant divergence incident slit is used, as opposed to the constant illuminated area system (theta-compensating slits); the changes required for the latter case are minor. In addition, the specimen will be assumed to be semi-infinite, i.e. larger than the x-ray footprint for all x-ray incidence angles, and thick enough that x-rays do not pass through it . These assumptions simplify the exposition of the theory without removing any of the essential details. The goal of the data analysis is to calculate the texture of the

specimen from the reduced (background subtracted) rocking curve, $I(2\theta_o, \alpha)$. Correction factors are applied to $I(2\theta_o, \alpha)$ to obtain the corrected rocking curve, $I_c(2\theta_o, \alpha)$, which has the shape of the texture profile over the α range measured. We define a function, $T(\alpha)$, which is proportional to the texture of the specimen such that:

$$I_c(2\theta_o, \alpha) = I(2\theta_o, 0) \quad T(\alpha), \tag{3}$$

and $T(0) = 1$, so that the reduced and corrected rocking curves have equal values at $\alpha = 0$ which facilitates graphical comparison. Note that $I(2\theta_o, 0)$ is both the maximum intensity of the peak profile and the rocking curve intensity at zero tilt; the agreement between these two measurements provides a consistency check between the two scans. The functional forms for $V(2\theta_o, \alpha)$ and $T(\alpha)$ are derived below.

The geometry of the diffraction setup is given in Fig. 1 which is a schematic of the diffraction plane of the diffractometer. The upper part of the figure shows a flat specimen, rotated α about the axis normal to the figure at O; note that counter-clockwise rotations are positive. The specimen is irradiated by a beam of constant divergence angle γ_i , and the diffractometer radius, defined as the distance from both the source (S) and the detector (D) to the rotation axis (O), is R_o. During the rocking curve measurement, the scattering angle is set to $2\theta_o$, the Bragg value for the planes whose texture is being investigated. The origin of an orthonormal basis is placed at O, with the x-axis parallel to the specimen surface and the z-axis normal to the specimen, as shown. The beam is from a line source and so the analysis in this paper is two-dimensional and considers only the diffraction plane ($y = 0$). Therefore, we assume for convenience that the beam dimension in the y direction is unity. The figure shows how, during the rocking curve scan, areas of the specimen become defocused when α and x are both non-zero, i.e. the scattering angle, $2\theta'$, varies along the irradiated area of the specimen from less than $2\theta_o$ ($2\theta_-$) at one end of the irradiated area, through $2\theta_o$ at the specimen rotation axis ($x = 0$), to greater than $2\theta_o$ ($2\theta_+$) at the other end. For an incident ray at angle γ from the central ray SO, the scattering angle $2\theta'(\theta, \alpha, \gamma)$ is given by simple geometry as:

$$2\theta'(\theta, \alpha, \gamma) \approx 2\theta + \frac{2 \sin\gamma \cos\theta}{\sin(\theta + \alpha - \gamma)} \left(\frac{\sin\gamma \sin\theta}{\sin(\theta + \alpha - \gamma)} - \sin\alpha \right), \tag{4}$$

where the first term in the parentheses relates to the flat specimen correction and the second term to the tilt. The ray at γ to SO is incident on the specimen surface at angle ϕ given by:

$$\phi = \theta + \alpha - \gamma. \tag{5}$$

The lower part of Fig. 1 shows the reduced θ-2θ scan of the peak. The peak is shown as a

singlet, i.e. a monochromatic radiation source, but the technique does not require that the incident beam be monochromatic. To calculate the effect of defocus, we consider that the beam (total width γ_i) is divided into elements of angular width $d\gamma$, which irradiate rectangular specimen elements with their length parallel to the specimen rotation axis. The x-ray intensity per radian in the diffraction plane is B. During the rocking curve measurement, the intensities diffracted by specimen elements not at the rotation axis are decreased because of defocus. The analysis in this section is based on the postulate that the defocus-induced variation in diffracted intensity from any point along the length of the specimen is given by the intensity distribution of the reduced θ-2θ scan of the peak, in the way illustrated by the dashed lines in Fig. 1. Another factor influencing the intensity of the raw rocking curve is variation in the attenuation caused by x-ray absorption in the specimen. The attenuation of a ray incident on the surface at angle ϕ that penetrates to depth z in the specimen, scatters through $2\theta'$ and returns to the surface, $K(z, \phi, 2\theta')$, is given by:

$$K(z, \phi, 2\theta') = \exp\left\{ -\mu z \left(\frac{1}{\sin\phi} + \frac{1}{\sin(2\theta' - \phi)} \right) \right\}, \qquad (6)$$

where μ is the linear coefficient of x-ray absorption.

The analysis given here follows in the spirit of Warren [8] who considered scattering of a beam of known intensity per unit area by a unit volume of specimen. The intensity per unit area of a divergent beam incident at distance R from the source is B / R, where B is the intensity per radian of the x-ray source in the diffraction plane. The volume of a specimen element dz thick irradiated by beam element $d\gamma$ at distance R from the source is $R\, d\gamma\, dz / \sin\phi$. We define the scattering power of the specimen material by considering unit volume of specimen to be irradiated by unit x-ray intensity per unit area: the x-ray intensity scattered by this volume through 2θ in the diffraction plane is $F(2\theta)$. Thus, the intensity scattered by a volume element irradiated by a beam element is $F(2\theta)\, B\, d\gamma\, dz / \sin\phi$. To find the intensity that is scattered from an element at depth z and exits the specimen in the direction of the detector we multiply by the attenuation factor $K(z, \phi, 2\theta')$. Finally, we apply the texture function $T(\alpha`(\alpha, \gamma))$, where $\alpha`(\alpha, \gamma)$ is the angle between the specimen normal and the scattering vector at the element. The variation of $\alpha`$ over $\gamma_i$ is small enough that $T(\alpha`)$ can be treated as constant and equal to $T(\alpha)$. This approximation is valid except in the case of very highly textured specimens (e.g. epitaxial systems, layered structures); however, in these cases, measurements are made over very small tilt ranges so that the errors introduced by defocussing are insignificant and do not require correction. The

intensity recorded at 2θ for a given value of α is calculated by integrating over the total irradiated volume, i.e. over the angular width of the beam, and the thickness of the specimen:

$$I(2\theta, \alpha) = B\ T(\alpha) \int_{-\gamma_i/2}^{\gamma_i/2} F(2\theta'(\theta, \alpha, \gamma)) \int_0^{\infty} \frac{K(z, \phi, 2\theta')}{\sin\phi}\ dz\ d\gamma. \tag{7}$$

Evaluating the integral over z gives:

$$I(2\theta, \alpha) = \frac{B\ T(\alpha)}{\mu} \int_{-\gamma_i/2}^{\gamma_i/2} \frac{\sin(2\theta' - \phi)}{\sin\phi + \sin(2\theta' - \phi)}\ F(2\theta'(\theta, \alpha, \gamma))\ \ d\gamma. \tag{8}$$

For the θ-2θ scan, α = 0, θ = φ and T(α) = 1. Over the range of the integral, 2θ′ varies only by the flat specimen correction, typically less than 0.01°, so that to a good approximation 2θ′ = 2θ and:

$$I(2\theta,\ 0) = \frac{B\ \gamma_i\ F(2\theta)}{2\ \mu}. \tag{9}$$

Substituting the expression for F(2θ) obtained from eqn. (9) into eqn. (8) gives a general expression for I(2θ, α) in terms of I(2θ, 0):

$$I(2\theta, \alpha) = \frac{T(\alpha)}{\gamma_i} \int_{-\gamma_i/2}^{\gamma_i/2} \frac{2\ \sin\ (2\theta' - \phi)}{\sin\phi + \sin\ (2\theta' - \phi)}\ \ I(2\theta'(\theta, \alpha, \gamma), 0)\ \ d\gamma. \tag{10}$$

In this equation, T(α) describes specimen texture, and the rest of the expression gives the intensity detected from the specimen, corrected for absorption, and averaged over the incident beam as shown pictorially in Fig. 1. Substituting T(α) derived from eqn. (10) into eqn. (3) gives the full expression for the corrections that must be applied to the measured rocking curve, $I(2\theta_o, \alpha)$, to obtain the corrected rocking curve, $I_c(2\theta_o, \alpha)$:

$$I_c(2\theta_o, \alpha) = I(2\theta_o, \alpha) \frac{I(2\theta_o, 0)\ \gamma_i}{\int_{-\gamma_i/2}^{\gamma_i/2} \frac{2\ \sin\ (2\theta' - \phi)}{\sin\phi + \sin\ (2\theta' - \phi)}\ \ I(2\theta'(\theta, \alpha, \gamma), 0)\ \ d\gamma}. \tag{11}$$

The background has been subtracted from the intensities in eqns. (10) and (11) using eqns. (1) and (2). The background factor in eqn. (2), V(2θ, α), is the ratio of $I_b(2\theta, 0)$ to $I_b(2\theta, \alpha)$, which can be calculated using eqn. (10). Considering background intensities, for all reasonable values of α and γ, T(0) = T(α) and $I_b(2\theta'(\theta, \alpha, \gamma), 0) = I_b(2\theta, 0)$ so that:

$$V(2\theta, \alpha) = \frac{\sin\ (\theta + \alpha) + \sin\ (\theta - \alpha)}{2\ \sin\ (\theta - \alpha)}. \tag{12}$$

The above theory has provided the computational basis of the software that has been written for the analysis of the x-ray data. The integrals in equations (10) and (11) are evaluated from the raw data

using Simpson's rule. In cases of axisymmetric texture, $I_c(2\theta_o, \alpha)$ is symmetrical about an α value near zero, α_m, and an overlap curve, $I_o(2\theta_o, \alpha)$, is calculated:

$$I_o(2\theta_o, \alpha) = \frac{I_c(2\theta_o, \alpha_m - \alpha) + I_c(2\theta_o, \alpha_m + \alpha)}{2}, \quad (13)$$

for analysis by curve-fitting procedures. The value of α_m observed experimentally was usually much less than 0.5°, reflecting the fact that the alignment of the fiber axis with the specimen normal was very good. As will be seen, even untextured materials give raw rocking curves that are noticeably peaked; the magnitude of the total correction factor in eqn. (11) can be significant (as high as 10) for large values of α and γ.

IV. VERIFICATION AND APPLICATIONS OF THE TECHNIQUE

The initial verification of the technique was carried out by analysis of a Standard Reference Material, a de-aggregated, equiaxed, alumina powder (SRM 676). This powder forms beds which have been shown to have no preferred orientation by Rietveld/March-Dollase analysis of a complete x-ray spectrum taken over a 2θ range from 20° to 154° [9]. The verification of the rocking curve technique employed both theta offset scans, to validate eqn. (10), and rocking curve analysis, to validate eqn. (11). Conventional scans (θ-2θ) were performed over the 03$\underline{3}$0 peak ($2\theta_o$ = 68.2°) using different theta offset values, α_o, of -15°, 0°, 15°, thus measuring $I(2\theta, \alpha_o)$ as the scattering angle 2θ was varied. Since untextured specimens were used for the θ-offset scans, $T(\alpha_o) = 1$ for any α_o, allowing direct comparison to be made between an experimental θ-offset scan and one calculated from the symmetric scan using eqn. (10). The incident slit size was 0.68° and the final slit size was 0.15° for all these scans. The 0° offset and -15° peaks, plotted in Fig. 2(a), show that the experimental -15° offset peak is considerably broader than the 0° peak, primarily because the irradiated area is much larger for -15° offset than 0°. Using eqn. (10) and the 0° offset scan for $I(2\theta, 0)$, the -15° offset scan was calculated and is plotted in Fig. 2(b) together with the experimental peak from Fig. 2(a). Figure 2(c) contains the experimental and calculated 15° offset peaks; the 15° peak is broader than the 0° peak but less broad than the -15° peak because the irradiated area decreases as α increases and so the defocus correction has less effect on the shape of the peak. The agreement between the experimental curves and the calculations shown in Figs. 2(b) and (c) is extremely good, indicating that the theory on which eqn. (10) is based is well-founded.

Raw rocking curve data were collected from SRM 676 using the 03$\underline{3}$0 alumina peak ($2\theta_o$ = 68.2°) for a variety of incident and receiving slit sizes; Figs. 3(a), (b) and (c) show the reduced and corrected rocking curves. For Fig. 3(a) the incident slit size (γ_i) was 0.68° and the receiving slit size (γ_r) was 0.15°; for Fig. 3(b) the incident slit was 0.23° and the receiving slit was 0.15°; for Fig. 3(c) the incident slit was 0.68° and the receiving slit was 0.60°. The corrected rocking curves were almost perfectly linear, and had slopes close to zero. They were fitted with linear functions which gave: for 3(a): $I_c(\alpha) = 943.5 - 0.1\alpha$ (i.e. the intensity was constant to ~0.01% per degree over the whole α range); for 3(b): $I_c(\alpha) = 293 + 0.6\ \alpha$ (i.e. constant to ~0.2% per degree); for 3(c): $I_c(\alpha) = 1121 + 0.34\ \alpha$ (i.e. constant to ~0.03% per degree). The differences between the reduced and corrected rocking curves were considerable in all cases which shows that the correction factor can become large (of the order of 10 or more) as α approaches θ_o.

Two BSCCO 2223 tape specimens (#1 and #2) displaying different levels of texture were analyzed using three different texture measurement methods: the corrected rocking curve (α scan) technique, chi (χ) scans, and pole figures. Each α scan was converted to an "overlap" curve using eqn.(13). For a χ scan, the specimen is placed in the symmetric diffraction orientation for a Bragg peak, and the peak intensity is measured while the specimen is rotated about an axis defined by the intersection of the specimen plane and diffraction plane. This axis is orthogonal to the α rotation axis, and for the measurement of diffracting planes parallel to the specimen surface, χ and α are equivalent. For χ angles up to approximately 50°, no defocussing correction is required. Pole figure data were collected using a 5° grid to measure the (00$\underline{2}$4), (105), and (219) poles for each sample. The orientation distribution function (ODF) was calculated but the pole figures reconstructed from the ODF were not used due to peak overlapping at higher tilt angles. Only the (00$\underline{2}$4) pole figure is used in the subsequent analysis; however, the (105) and (219) as-measured pole figures do confirm the texture is axisymmetric about [001]. The measured (00$\underline{2}$4) pole figures were corrected for background and defocussing with a randomly textured sample, then averaged over the angle ϕ, which represents a rotation about the sample normal.

Figures 4(a) and 4(b) show the results of these experiments, plotted out to 30° in α and χ. Since the α and χ scans and the corrected pole figures are in arbitrary units of diffracted intensity, the three

curves can be scaled in intensity to allow comparisons; it is clear that the shape and the full-width at half maximum (FWHM) of these plots are similar, with the curves for wire #1 nearly identical (Fig. 4(a)). The FWHMs of wires #1 and #2 are 21.1° and 16.5° respectively, signifying a sharper [001] or c-axis texture for wire #2.

As part of the verification process, this texture analysis technique has been implemented on different conventional powder x-ray diffractometers at NIST and American Superconductor Corporation. Texture data collected from the same BSCCO specimen at both sites were virtually identical and gave FWHM values that differed by 0.3° or less.

V. DISCUSSION

For clarity, the theory presented above has assumed that the specimen is semi-infinite. The software has been developed for the more general case of a sample of finite area. However, there are still restrictions on the geometry of the specimen: 1) the specimen must be x-ray opaque, and the scattering power, $F(2\theta)$, and texture of the specimen must be homogeneous; 2) either a) the diffracting area of the specimen must be larger than the x-ray footprint over the α range used, or b) it must have at least two orthogonal mirror planes (e.g. a rectangle), with one of its mirror planes mounted in the diffraction plane. Requirement (1) limits the technique to homogeneous bulk specimens. Application to thin films requires modification of the theory and software. This has been recently carried out and the results will be published soon. In case (2a), the diffracting area of the specimen is large enough that the scans can be recorded with or without the sample spinning. If the sample spinner is used, information about lack of axisymmetry in texture is lost. In case (2b), the scans must be recorded without rotating the specimen, and the dimensions of the specimen must be measured.

For the SRM 676 measurements, the specimen was sufficiently large that requirement 2a was satisfied. Data were collected with and without the sample spinning, and no detectable differences were observed between the corrected rocking curves. In the BSCCO experiments, the specimens were rectangular and were usually mounted with the longer axis lying in the diffraction plane, thus measuring texture in the plane defined by this axis and the specimen normal. By turning the specimen through 90°, texture was also measured in the orthogonal plane containing the specimen normal, and information on the degree of texture axisymmetry was obtained. Scans at intermediate “phi” angles would allow measurement of a detailed pole figure in the region of orientation space defined by the

accessible range of α.

The similarities between the experimental and calculated theta offset curves in Figs. 2(b) and (c) and the relatively flat corrected rocking curves in Fig. 3 indicate that implementation of the theory given in this paper successfully corrects rocking curves measured with a powder diffractometer and yields accurate texture measurements. However, the results do not indicate perfect agreement in Figs. 2 or corrected curves of zero slope in Figs. 3. It is useful to conjecture on the reasons for this, and consider various options for refining the technique. The size of the incident slit is a variable in the theory that must be known to enable accurate corrections to the raw data to be made. Even more precise corrections could be made if the intensity profile of the incident beam were measured as a function of γ. These data could be easily incorporated into the calculation of $I_c(2\theta_o, \alpha)$ using a slightly modified version of eqn. (11). A number of assumptions were made in the derivation of eqns. (9), (10) and (11), and neglect of the flat specimen correction in eqn.(9) may contribute to the discrepancy just noted. Alternatively, the SRM 676 specimen may not conform to the requirements 1 and 2 above; for example the powder bed may not be perfectly homogeneous. The receiving slit size does not enter into the theory or the calculations, because it is assumed that the peak profile describes the variation with scattering angle of the intensity diffracted by each volume element of specimen *for the same size receiving slit.* The validity of this assumption can be seen from Figs. 3(a) and (c) where the size of the receiving slit does not significantly influence the shape of the corrected rocking curves. However, there may be subtle interactions between the flat specimen correction and the size of the receiving slit which have not as yet been explored.

Considering the data presented in Fig. 4, there are strengths and limitations to the three techniques employed. One of the main strengths of the rocking curve technique is that it does not require an untextured (or random) specimen of the material; the other two techniques do. Obtaining truly random specimens and verifying that they are random is difficult. Common to most x-ray texture measurements is the problem of peak overlap where the peak being used for the measurement lies close to other diffraction peaks from the specimen. Peak overlap is likely to be a larger problem for the method described in this paper than for the pole figure and χ scan methods because relatively large beam divergences are used, which results in large defocus values and increased interference from neighboring peaks. The interfering peaks may not be apparent at zero tilt where the measurement peak is often very strong. For textured specimens, as the tilt increases, the intensity of the measurement peak

decreases while the intensity of the interfering peak grows. When using the rocking curve technique, the presence of interfering peaks can be investigated using theta offset scans over the measurement peak (as in Fig. 2). If the shapes of the experimental and calculated theta offset peaks do not match well for any value of T(α), it is likely that there are problems with peak overlap.

The data collection time for a rocking curve measurement was always less than 60 minutes and could be as little as 20 minutes. The slit sizes used were large enough that the signal to noise level was high. The χ scan data collection can be accomplished relatively quickly, but the incident slit is small to reduce defocussing corrections to a minimum and therefore the signal is typically relatively weak and noisy. The pole figure approach provides the most complete texture measurement of the three, but like the χ scan it requires a considerably larger investment in instrumentation. The size of the region of orientation space that can be investigated using the rocking curve technique depends on the Bragg angle of the peak used for the texture measurement. Typically we select the highest angle peak from the textured planes that has adequate intensity; for BSCCO 2223 the 00<u>24</u> peak, with a Bragg angle of 59.8°, was used. With this peak, the usable BSCCO rocking curve data only extended to 24° in α, but the data were collected at a high density of data points per degree, whereas the pole figure data are two-dimensional and extend to 80° in χ, but only at increments of 5° in χ. An extension to the rocking curve technique is planned where data are collected using reciprocal lattice vectors not parallel to the preferred crystallographic direction. Thus texture measurements over a larger region of orientation space could be made.

While pole figure data can be expressed in units of MRD, rocking curve data only cover a limited region of orientation space. Therefore, they can only be normalized for conversion to MRD by fitting a function to the limited data set and extrapolating to the whole orientation space, a procedure which yields very unreliable MRD results. Thus, MRDs cannot be obtained from the rocking curves presented in this paper (or from χ scans); however, full width at half maximum (FWHM) values of the corrected rocking curves can be measured accurately. Also, since the density of data points in the corrected rocking curves is high, texture models can be fitted to the data and the degree of fit can be determined with confidence.

VI. CONCLUSIONS

The texture measurement technique described in this paper requires only a conventional powder

diffractometer, and it is relatively fast. The raw rocking curve intensities are corrected for defocussing using the intensity profile of the measurement peak. The method has been validated with measurements on untextured alumina (SRM676) with the following results: 1) calculated and experimental theta offset peak profiles agreed extremely well; 2) the magnitude of corrected rocking curves varied very little with tilt angle. Application of the technique was made to BSCCO tapes, and agreement between rocking curves, χ scans and pole figures was excellent.

Appendix

Software has been developed to do corrected rocking curve and theta offset curve calculations. The software is capable of analyzing data from thin films, which requires the film thickness and the linear coefficient of x-ray absorption as additional data. It employs a convenient graphical user interface and is available on written request from Mark Vaudin (email: mark.vaudin@nist.gov, fax: 301-975-5334)

Acknowledgements

The authors would like to acknowledge Dr. Qi Li at American Superconductor Corporation for supplying the samples used in the BSCCO study. In addition, a number of the authors benefited from discussion with members of the Wire Development Group, especially David Larbalestier (University of Wisconsin at Madison), Terry Holesinger and Jeff Willis (Los Alamos National Laboratory), Don Kroeger (Oak Ridge National Laboratory), Vic Maroni (Argonne National Laboratory), Steve Freiman (National Institute of Standards and Technology), and Qi Li and Ron Parrella (American Superconductor Corporation).

References

1. *Powder Diffraction File*, International Center for Diffraction Data, Newtown Square, PA, 1996.
2. S. Martin, A.T. Fiory, R.M. Fleming, G.P. Espinosa and A.S. Cooper, Appl. Phys. Letts 54, 72 (1989).
3. “Anisotropy of critical current density in Bi-2223/Ag tapes.”, C. Takahashi, M. Nagano, Y.Wakiya, T. Kato, K. Sato, Advances in Superconductivity VII. Proceedings of the 7th International Symposium on Superconductivity (1995).
4. F.K. Lotgering, J. Inorg. Nucl. Chem. 9, 113 (1959).
5. J.P. Cline, M.D. Vaudin, J.E. Blendell, C.A. Handwerker, R. Jiggets, K.J. Bowman and N.

Medendorp, Advances in X-Ray Analysis 37, 473 (1994).

6. E. Tenckoff, J. Appl. Phys. 41, 3944 (1970).

7. E.M.C. Huijser-Gerits and G.D. Rieck, J. Appl. Cryst. 7, 286 (1974).

8. B.E. Warren, X-Ray Diffraction (Dover Publications, New York, 1990), chapter 4.

9. W. Kalceff, J.P. Cline and R.B. VonDreele, Advances in X-ray Analysis 31, 343 (1994).

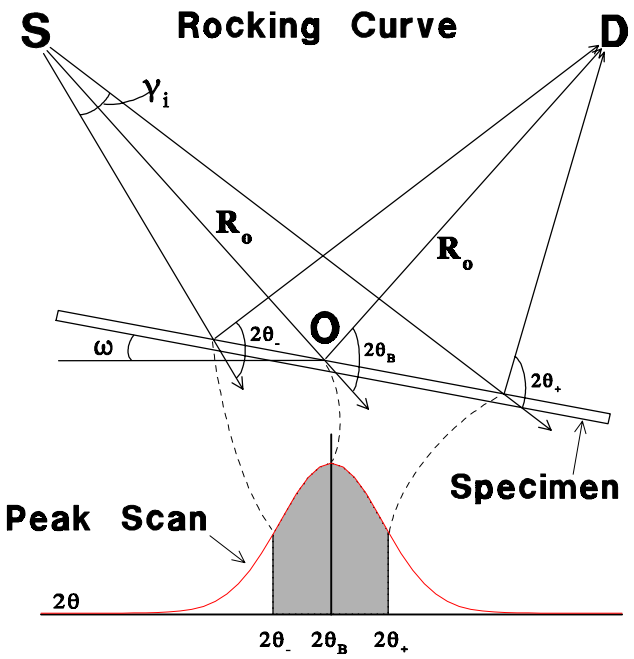

Figure 1. Schematic of rocking curve geometry showing relationship between specimen defocus (top) and peak profile (bottom). Beam divergence is greatly exaggerated for illustration purposes.

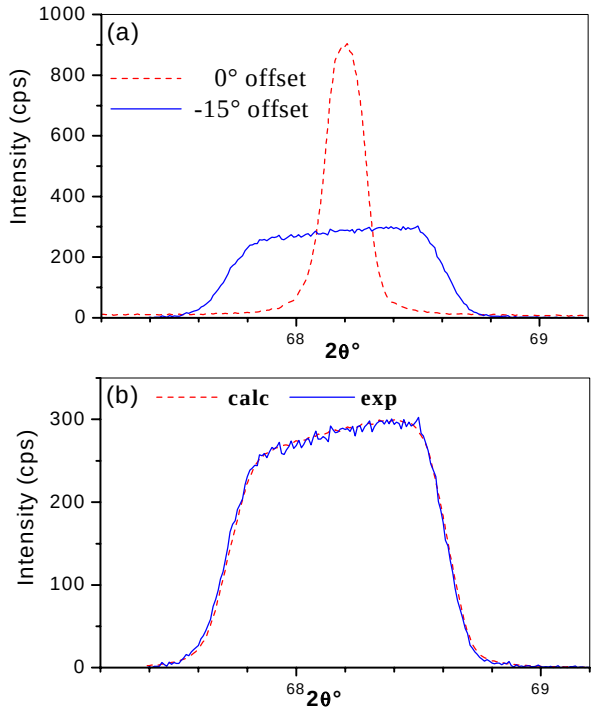

Figure 2. Theta offset peaks from SRM 676: (a) experimental 0° and -15° curves; (b) experimental and calculated -15° curves; (c) experimental and calculated 15° curves.

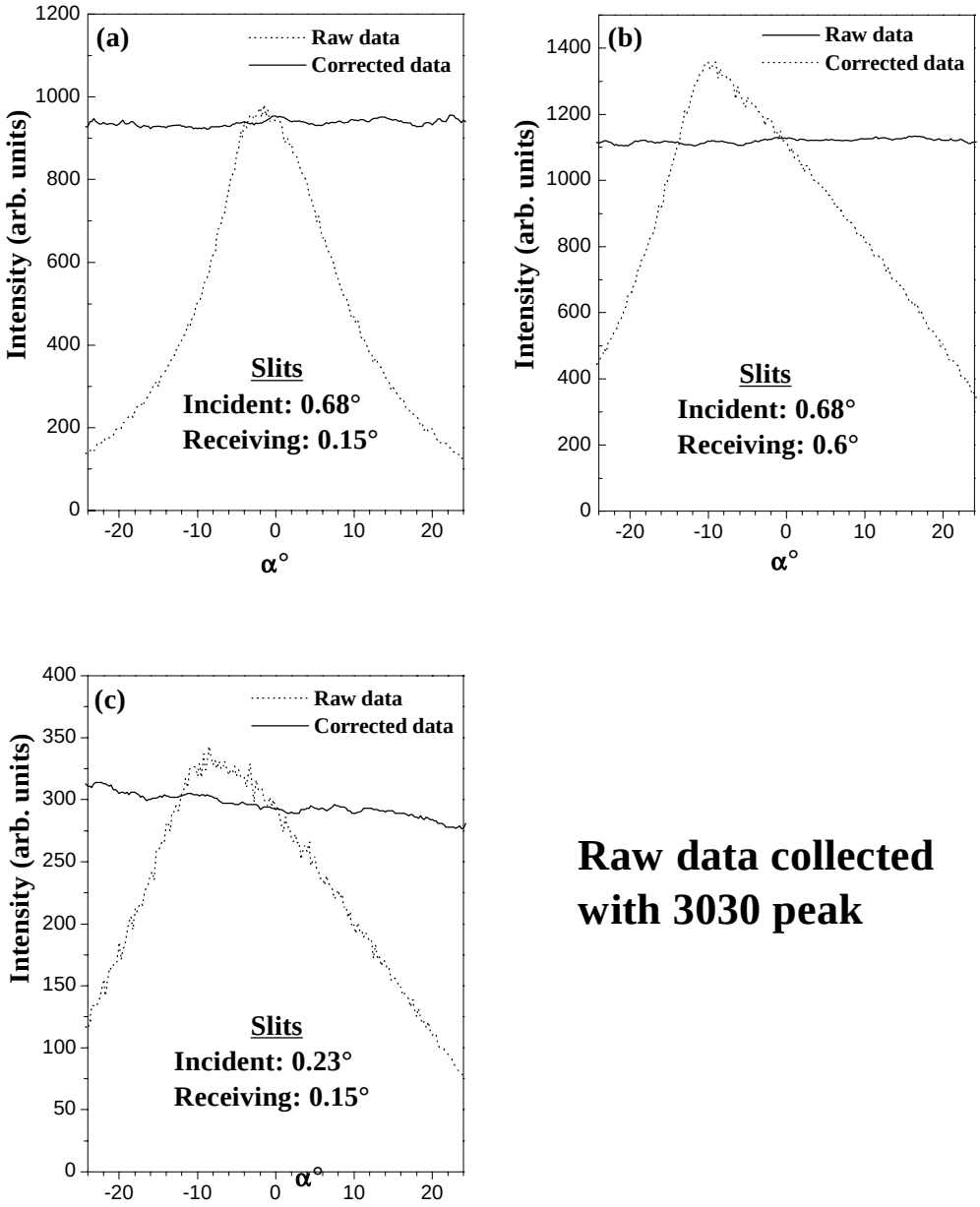

Fig. 3: Raw and corrected rocking curves from untextured alumina (SRM676) with different incident and receiving slits; (a) $\gamma_i = 0.68°$, $\gamma_r = 0.15°$; (b) $\gamma_i = 0.68°$, $\gamma_r = 0.6°$; (c) $\gamma_i = 0.23°$, $\gamma_r = 0.15°$.

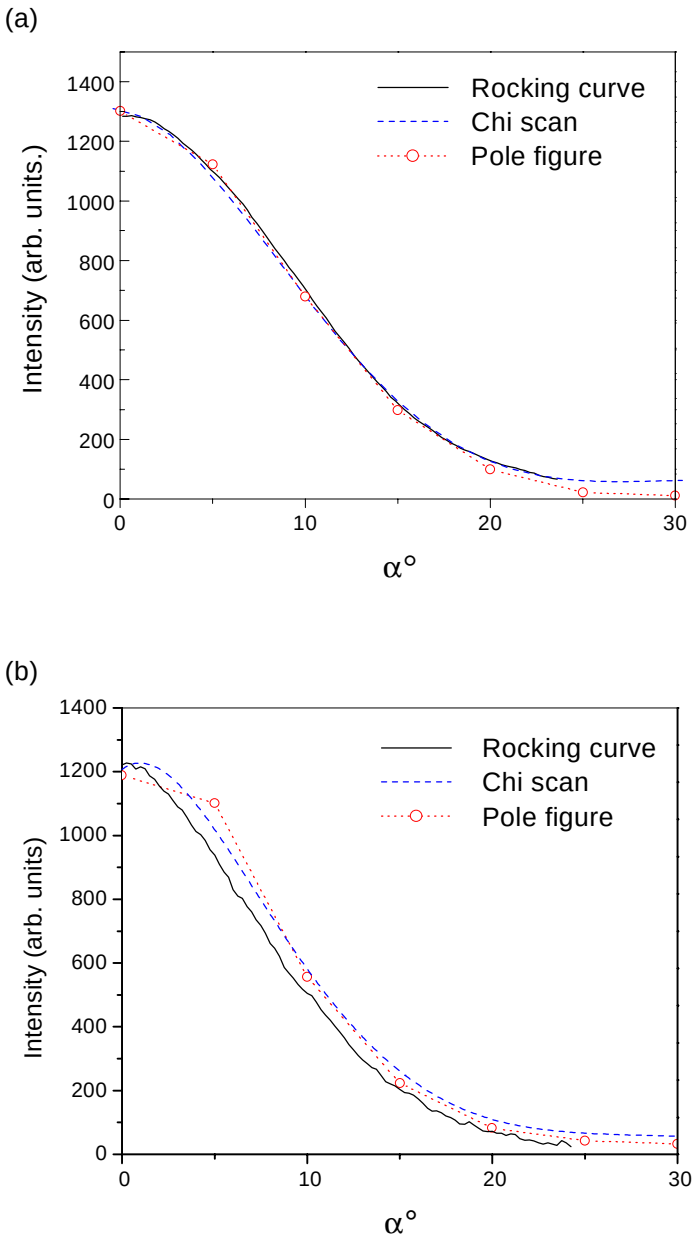

Figures 4(a) and (b). Texture measurements from two BSCCO wire specimens using rocking curves, χ scans and pole figures.